

Fast and accurate modeling of waveguide grating couplers

P. G. Dinesen

Dept. of Optics and Fluid Dynamics, Risø National Laboratory
DK-4000 Roskilde, Denmark

J. S. Hesthaven

Division of Applied Mathematics, Brown University, Box F
Providence, Rhode Island 02912

March 15, 2000

Abstract

A boundary variation method for the analysis of both infinite periodic and finite aperiodic waveguide grating couplers in 2-D will be introduced. Based on a previously introduced boundary variation method for the analysis of metallic and transmission gratings a numerical algorithm suitable for waveguide grating couplers is derived. Examples of the analysis of purely periodic grating couplers are given illustrating the convergence of the scheme. An analysis of the use of the proposed method for focusing waveguide grating couplers is given, and a comparison with a highly accurate spectral collocation method yields excellent agreement and illustrates the attractiveness of the proposed boundary variation method in terms of speed and achievable accuracy.

1 Introduction

In recent years, an increasing interest in the design and use of diffraction based integrated optics has lead to a need for fast and accurate numerical methods for the analysis and design of diffraction dominated structures. The formulation and development of such methods are severely complicated by the rigorous treatment of the vector-field behavior in the resonant regime where the wavelength of the optical field is comparable to the size of the geometrical features.

For inherently periodic structures of infinite extend, the rigorous coupled-wave analysis has been widely used for more than a decade[1]. However, the

need to analyze structures with aperiodic features and of finite extent has lead to the need for methods capable of dealing with such structures, and the use of the Finite-Element[2], Boundary element[3], Finite-Difference Time-Domain[4, 5], and Spectral Collocation[6] methods has been proposed. The latter two methods both compute a direct solution of the time-domain vectorial Maxwell equations and are very general in being adaptable to a wide variety of geometries and physical settings. As the need to model problems of realistic size and complexity becomes more pressing, however, the memory and computational time requirements of such direct volume methods quickly becomes a limiting factor not only for the design process but also for the analyses of particular structures.

In this work, we propose to take a different road, guided by the work of Bruno and Reitich[7]. They have established that solutions to electromagnetic diffraction by a periodic structure depend analytically on the variations of the interface. In other words, diffraction from a periodic grating can be determined from knowledge of reflection and refraction at a plane interface. Using this result, Bruno and Reitich proposed a high-order perturbation scheme for finite-size perturbations and successfully used it in modeling diffraction by two and three-dimensional metallic and transmission gratings[8, 9].

In this paper, we propose a further development leading to a formulation for the analysis of waveguide grating couplers, in which a guided wave in a thin-film waveguide is coupled to free-space radiation through a surface relief as sketched in Fig. 1. Moreover, we extend the analysis to structures of finite extent and demonstrate, by comparison with a highly accurate spectral collocation method, that the method of boundary variation provides surprisingly accurate results for the modeling of radiation from waveguide grating couplers.

The remainder of this paper is organized as follows. In section 2 we present the modified boundary variation method as applied to the waveguide grating coupler and discuss the details of the numerical implementation including post processing by free-space integration of the radiated field. Section 3 demonstrates the use of the proposed code for the analysis of periodic waveguide grating couplers, and in section 4 we subsequently turn to the analysis of finite-length focusing grating couplers with an aperiodic grating function. We present a comparison of the proposed method with a spectral collocation code to demonstrate the accuracy the boundary variation method for the modeling of nontrivial waveguide grating couplers. We conclude with a discussion of the superior computational efficiency of the proposed approach, and a few remarks of future directions of work.

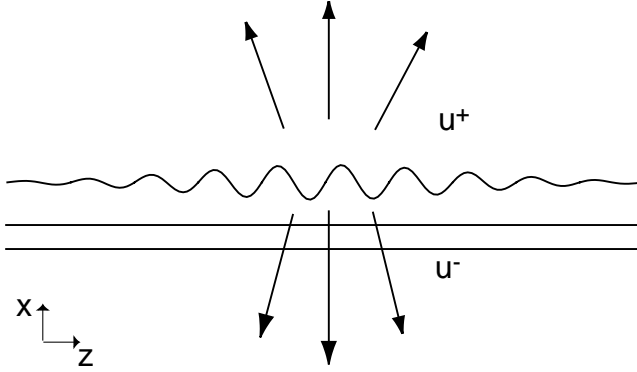


Figure 1: Thin-film optical waveguide comprising surface relief grating for coupling from guided wave to free-space radiation.

2 Boundary variation for grating couplers

In the following, we shall outline the elements of the proposed algorithm without going into details with the algebra involved in the derivation of the scheme but rather dwell on the properties of a field propagating in a thin film waveguide. It is an understanding of these properties that allows us to develop a method of boundary variation suitable for waveguide grating couplers based on the method for periodic dielectric interfaces[8].

We restrict ourselves to the analysis of TE polarized, monochromatic fields in which case the E field remains parallel to the grating, $\mathbf{E} = E_y \hat{y}$ and therefore is determined by a single scalar quantity, $u = u(z, x)$, satisfying the homogeneous Helmholtz equation

$$\Delta u + k^2 u = 0, \quad (1)$$

with k being the local wavenumber. We distinguish between the field that is radiated into the free space above the grating coupler, u^+ , and the field radiated downwards into the waveguide, u^- , as illustrated in Fig. 1.

We furthermore assume that the incident field is given by the fundamental TE mode for the unperturbed thin film waveguide. For a multi-layer waveguide the field in each individual layer is given on the form

$$E_i = A_i \exp(ik_i x - i\beta z) + B_i \exp(-ik_i x - i\beta z), \quad (2)$$

where k_i is given by

$$k_i^2 + \beta^2 = n_i^2 k_0^2, \quad (3)$$

with k_0 being the free-space wave number, while β is the propagation constant, determined by the layer thicknesses and the refractive indices[10]. A_i and B_i in Eq. (2) are constants, which are given once the propagation constant is calculated.

The TM case can be solved in a similar way using H_x rather than E_y . Although the boundary conditions will be different, the extension to the TM case is straightforward.

2.1 Numerical algorithm

Let us now consider the case where the boundary between the top cladding layer and free-space above the waveguide is perturbed in a way described by the function f and a real number δ , such that

$$x = f_\delta(z) = \delta f(z) \quad (4)$$

describes the upper surface of the top cladding layer. Assuming that the incoming field takes the form in Eq. (2), the radiation fields u^+ and u^- must satisfy the continuity conditions

$$\begin{aligned} u^+ - u^- &= A_0 \exp(ik_0\delta f(z) - i\beta z) + B_0 \exp(-ik_0\delta f(z) - i\beta z) \\ &\quad - A_1 \exp(ik_1\delta f(z) - i\beta z) - B_1 \exp(-ik_1\delta f(z) - i\beta z), \end{aligned} \quad (5)$$

and

$$\begin{aligned} \frac{\partial u^+}{\partial n} - \frac{\partial u^-}{\partial n} &= \frac{\partial}{\partial n} (A_0 \exp(ik_0\delta f(z) - i\beta z) + B_0 \exp(-ik_0\delta f(z) - i\beta z)) \\ &\quad - \frac{\partial}{\partial n} (-A_1 \exp(ik_1\delta f(z) - i\beta z) - B_1 \exp(-ik_1\delta f(z) - i\beta z)), \end{aligned} \quad (6)$$

at $x = \delta f(z)$. By requiring that the field vanishes for $x \rightarrow \infty$, we have $A_0 = 0$.

The central idea underlying the boundary variation method is that the radiated fields u^+ and u^- can be expanded in powers of δ

$$u^\pm(z, x, \delta) = \sum_{n=0}^{\infty} u_n^\pm(z, x) \delta^n. \quad (7)$$

Bruno and Reitich established the validity of this power series expansion, which is a result of u^\pm being analytic in its variables[11]. u , being a solution to the Helmholtz equation, can be expanded in a Rayleigh series

$$u^\pm(z, x, \delta) = \sum_{r=-\infty}^{\infty} B_r^\pm(\delta) \exp(i \pm \alpha_r^\pm x - i\beta_r z). \quad (8)$$

and likewise for the u_n^\pm

$$u_n^\pm(z, x) = \sum_{r=-\infty}^{\infty} d_{n,r}^\pm \exp(\pm i\alpha_r^p m x - i\beta_r z), \quad (9)$$

Given

$$d_{n,r}^\pm = \frac{1}{n!} \frac{d^n B_r^\pm}{d\delta^n}(0), \quad (10)$$

we recover the power series expansion

$$B_r^\pm(\delta) = \sum_{n=0}^{\infty} d_{n,r}^\pm \delta^n. \quad (11)$$

for the Rayleigh coefficients B_r^\pm . To obtain the coefficients in this power series expansion, we need the Fourier expansions

$$\frac{f^l(z)}{l!} = \sum_{r=-lF}^{lF} C_{l,r} \exp(iK r x), \quad (12)$$

for $f^l/l!$ for l up to some N . In Eq. (12), K represents the smallest grating vector, we wish to resolve. For a periodic cosine surface relief, K is simply the grating wavenumber, $K = 2\pi/\Lambda$, where Λ is the period of the grating. For that case, the Fourier expansions need only extend to $F = 1$. In the case of an aperiodic grating of finite length $K = 2\pi/L$ where L is the total length of the computational domain.

The wavevectors for the diffracted fields are given by

$$\beta_r = \beta + nK, \quad (13)$$

and

$$(\alpha_r^\pm)^2 + \beta_r^2 = (k_i)^2 \quad (14)$$

where $i = 0$ for the α_r^+ and $i = 1$ for the α_r^- . Only a finite number of Rayleigh modes B_r^\pm will be propagating, since α_r 's will have non-zero imaginary parts for large r .

The derivation of the recursive expressions for $d_{n,r}$ is thoroughly described in [8] for diffraction at an interface between two dielectrics. In this work, we need to modify the original derivation by using the boundary conditions for a grating coupler, Eqs. (5)-(6).

To proceed, we perform an n times differentiation of the boundary conditions, Eqs. (5)-(6), with respect to δ and evaluate this at $\delta = 0$. For Eq. (5) this yields

$$\sum_{k=0}^n \frac{f(z)^{n-k}}{(n-k)!} \left[\frac{\partial^{n-k}}{\partial x^{n-k}} \left(\frac{1}{k!} \frac{\partial^k u^+}{\partial \delta^k} \right) (z, 0, 0) - \frac{\partial^{n-k}}{\partial x^{n-k}} \left(\frac{1}{k!} \frac{\partial^k u^-}{\partial \delta^k} \right) (z, 0, 0) \right] = (-B_0(ik_0)^n + A_1(-ik_1)^n + B_1(ik_1)^n) f(z)^n \exp(-i\beta z). \quad (15)$$

With

$$n_\delta = \frac{1}{(1 + \delta^2 f'(z)^2)^{1/2}} (-\delta f'(z), 1) \quad (16)$$

n differentiations of Eq. (6) with respect to δ , evaluated at $\delta = 0$, yields

$$\begin{aligned} & \sum_{k=0}^n \frac{f(z)^{n-k}}{(n-k)!} \left[\frac{\partial^{n-k+1}}{\partial x^{n-k+1}} \left(\frac{1}{k!} \frac{\partial^k u^+}{\partial \delta^k} \right) (z, 0, 0) - \frac{\partial^{n-k+1}}{\partial x^{n-k+1}} \left(\frac{1}{k!} \frac{\partial^k u^-}{\partial \delta^k} \right) (z, 0, 0) \right] \\ & - \sum_{k=0}^{n-1} \frac{f'(z) f(z)^{n-k-1}}{(n-k-1)!} \left[\frac{\partial^{n-k}}{\partial x^{n-k-1} \partial z} \left(\frac{1}{k!} \frac{\partial^k u^+}{\partial \delta^k} \right) (z, 0, 0) - \frac{\partial^{n-k}}{\partial x^{n-k-1} \partial z} \left(\frac{1}{k!} \frac{\partial^k u^-}{\partial \delta^k} \right) (z, 0, 0) \right] \\ & = \frac{1}{n!} [-B_0(i\beta n(ik_0)^{n-1} f'(z) f(z)^{n-1} + (ik_0)^{n+1} f(z)^n) \\ & \quad + A_1(i\beta n(-ik_1)^{n-1} f'(z) f(z)^{n-1} - (-ik_1)^{n+1} f(z)^n) \\ & \quad + B_1(i\beta n(ik_1)^{n-1} f'(z) f(z)^{n-1} + (ik_1)^{n+1} f(z)^n)] \exp(-i\beta z). \quad (17) \end{aligned}$$

From Eq. (7) we recover

$$u_k^\pm(z, x) = \frac{1}{k!} \frac{\partial^k u^\pm}{\partial \delta^k}(z, x, 0) \quad (18)$$

such that Eqs. (15) and (17) gives

$$\begin{aligned} u_n^+ - u_n^- &= [-B_0(ik_0)^n + A_1(-ik_1)^n + B_1(ik_1)^n] f(z)^n \exp(-i\beta z) \\ & - \sum_{k=0}^{n-1} \frac{f(z)^{n-k}}{(n-k)!} \left[\frac{\partial^{n-k} u_k^+}{\partial x^{n-k}} - \frac{\partial^{n-k} u_k^-}{\partial x^{n-k}} \right], \quad (19) \end{aligned}$$

and

$$\begin{aligned} \frac{\partial u_n^+}{\partial x} - \frac{\partial u_n^-}{\partial x} &= \\ & \frac{1}{n!} [-B_0(i\beta n(ik_0)^{n-1} f'(z) f(z)^{n-1} + (ik_0)^{n+1} f(z)^n) \\ & \quad + A_1(i\beta n(-ik_1)^{n-1} f'(z) f(z)^{n-1} - (-ik_1)^{n+1} f(z)^n) \end{aligned}$$

$$\begin{aligned}
& + B_1(i\beta n(ik_1)^{n-1}f'(z)f(z)^{n-1} + (ik_1)^{n+1}f(z)^n) \exp(-i\beta z) \\
& + \sum_{k=0}^{n-1} \frac{f'(z)f(z)^{n-k-1}}{(n-k-1)!} \left[\frac{\partial^{n-k} u_k^+}{\partial x^{n-k-1} \partial z} - \frac{\partial^{n-k} u_k^-}{\partial x^{n-k-1} \partial z} \right] \\
& - \sum_{k=0}^{n-1} \frac{f(z)^{n-k}}{(n-k)!} \left[\frac{\partial^{n-k+1} u_k^+}{\partial x^{n-k+1}} - \frac{\partial^{n-k+1} u_k^-}{\partial x^{n-k+1}} \right]. \tag{20}
\end{aligned}$$

By substituting the Rayleigh expansions for u_n^\pm , Eq. (9), into Eq. (19), we recover the coefficients $d_{n,r}$ from a recurrence in $d_{k,r}$, $k < n$ and from the Fourier coefficients $C_{k,r}$, on the form

$$\begin{aligned}
& \sum_{r=-\infty}^{\infty} (d_{n,r}^+ - d_{n,r}^-) \exp(-i\beta_r z) \\
& = (-B_0(ik_0)^n + A_1(-ik_1)^n + B_1(ik_1)^n) \sum_{r=-nF}^{nF} C_{n,r} \exp(-i\beta_r z) \\
& - \sum_{k=0}^{n-1} \left[\sum_{r=-(n-k)F}^{(n-k)F} C_{n-k,r} \exp(iKr z) \right] \\
& \times \left\{ \sum_{r=-\infty}^{\infty} [(i\alpha_r^+)^{n-k} d_{k,r}^+ - (-i\alpha_r^-)^{n-k} d_{k,r}^-] \exp(i\beta_r z) \right\}, \tag{21}
\end{aligned}$$

In a similar fashion, substituting Eq. (9) into Eq. (20) yields

$$\begin{aligned}
& \sum_{r=-\infty}^{\infty} (i\alpha_r^+ d_{n,r}^+ + i\alpha_r^- d_{n,r}^-) \exp(-i\beta_r z) \\
& = \sum_{r=-nF}^{nF} C_{n,r} [-B_0(i\beta(ik_0)^{n-1}(iKr) + (ik_0)^{n+1}) \\
& + A_1(i\beta(-ik_1)^{n-1}(iKr) - (-ik_1)^{n+1}) \\
& + B_1(i\beta(ik_1)^{n-1}(iKr) + (+ik_1)^{n+1})] \exp(-i\beta_r z) \\
& + \sum_{k=0}^{n-1} \left[\sum_{r=-(n-k)F}^{(n-k)F} C_{n-k,r} iKr \exp(iKr z) \right] \\
& \times \left\{ \sum_{r=-\infty}^{\infty} [(i\alpha_r^+)^{n-k-1} (-i\beta_r) d_{k,r}^+ - (-i\alpha_r^-)^{n-k-1} (-i\beta_r) d_{k,r}^-] \exp(-i\beta_r z) \right\} \\
& - \sum_{k=0}^{n-1} \left[\sum_{r=-(n-k)F}^{(n-k)F} C_{n-k,r} \exp(iKrx) \right]
\end{aligned}$$

$$\times \left\{ \sum_{r=-\infty}^{\infty} [(i\alpha_r^+)^{n-k+1} d_{k,r}^+ - (-i\alpha_r^-)^{n-k+1} d_{k,r}^-] \exp(-i\beta_r z) \right\}. \quad (22)$$

After some manipulations, utilizing that $d_{k,q}^{\pm} = 0$ for $|q| > kF$, we recover following recursive formulas for the coefficients $d_{n,r}^{\pm}$

$$\begin{aligned} d_{n,r}^+ - d_{n,r}^- &= (-B_0(ik_0)^n + A_1(-ik_1)^n + B_1(ik_1)^n)C_{n,r} \\ &\quad - \sum_{k=0}^{n-1} \sum_{q=\max[-kF, r-(n-k)F]}^{\min[kF, r+(n-k)F]} C_{n-k, r-q} [(i\alpha_q^+)^{n-k} d_{k,q}^+ - (-i\alpha_q^-)^{n-k} d_{k,q}^-] \\ i\alpha_r^+ d_{n,r}^+ + i\alpha_r^- d_{n,r}^- &= (-B_0(ik_0)^{n-1}[\beta Kr + (ik_0)^2] \\ &\quad + A_1(-ik_1)^{n-1}[\beta Kr + (-ik_1)^2] + B_1(ik_1)^{n-1}[\beta Kr + (ik_1)^2])C_{n,r} \\ &\quad + \sum_{k=0}^{n-1} \sum_{q=\max[-kF, r-(n-k)F]}^{\min[kF, r+(n-k)F]} C_{n-k, r-q} \{ [iK(r-q)] \\ &\quad \times (-i\beta_q) [(i\alpha_q^+)^{n-k-1} d_{k,q}^+ - (-i\alpha_q^-)^{n-k-1} d_{k,q}^-] \\ &\quad - [(i\alpha_q^+)^{n-k+1} d_{k,q}^+ - (-i\alpha_q^-)^{n-k+1} d_{k,q}^-] \}. \end{aligned} \quad (24)$$

Once the power series expansion coefficients, $d_{n,r}^{\pm}$, are determined, the Rayleigh expansion coefficients, B_r^{\pm} may be computed from the power series, Eq. (11). The radius of convergence, however, of this Taylor series is rather small. To overcome this, we recast, as suggested in [8], the expansion as a Padé approximation which significantly enhances the radius of convergence. We find that in general using an [M/M] approximant, i.e., using the same order of the polynomial in the numerator and denominator, yields the fastest convergence for our problem. As for the computation of the Fourier spectrum of the surface relief $f(z)$, Eq. (12), we use the Fast Fourier Transform (FFT) for enhanced computational speed.

It is important to observe that for the analysis of grating couplers, the boundary variation method is approximate as it does not account for the attenuation of the guided wave caused by the loss of energy by coupling to free-space. Furthermore, the method does not account for any reflections at lower lying boundaries of the downward radiation that is also subsequently coupled to free space. As we shall demonstrate, however, the method provides highly accurate solutions to simple as well as non-trivial test problems.

2.2 Post-processing

In principle, the diffracted field can be recovered anywhere above the grating coupler from the Rayleigh series expansion, Eq. (8), directly. However, due to the periodicity inherently assumed in the formulation of the scheme, we find it more convenient to evaluate the diffractive field along an aperture covering the grating coupler and use this field to recover the near- and farfield radiation from the structure through the use of the surface-equivalence theorem[12]. To maintain a high accuracy we compute the diffracted field on a set of quadrature points on which high-order integration can be performed.

3 Analysis of period grating couplers

In the following, we shall demonstrate the convergence of the proposed scheme for purely periodic gratings of infinite extent and give further examples of the analysis facilitated by the proposed method.

In the following all length parameters are normalized with the free-space wavelength λ of the incident field.

As the basic waveguide geometry for the numerical examples, we consider a waveguide structure consisting of a core layer with refractive index $n = 1.45$ and thickness $d_1 = 0.8$, sandwiched between two cladding layers of refractive index $n = 1.4$. The top cladding layer has a finite thickness of $d_2 = 1$ and above this layer is air with $n = 1$. For the fundamental TE mode this geometry yields an effective index of 1.4213.

We consider a cosine surface relief

$$f_\delta(z) = A \cos\left(\frac{2\pi}{\Lambda}z\right) \quad (25)$$

Let us first study the convergence of the scheme. As we do not have an analytic solution to compare with, we are unable to compute the error. Rather, we look at the power coupled to the -1st diffraction order as we increase the number of terms in the Padé approximation to the Taylor series expansion, Eq. (11). Table 1 confirms the convergence in the case of $A = 0.1$ as the number of terms in the power series expansion increases.

To investigate the sensitivity of the convergence further, we consider the convergence for increasing amplitudes of the surface relief. As we increase A , the error of the scheme increases in the sense that the number of significant digits for \bar{P} decreases. To give an estimate of the error, we compute the average and the standard deviation for M ranging from 15 to 49 for increasing

M	$\bar{P} (\cdot 10^{-2})$
2	1.208589
3	1.218618
4	1.220834
5	1.220240
6	1.220247
7	1.220242
8	1.220243
9	1.220243
10	1.220243

Table 1: Power in the -1st diffraction order for different number of terms [M,M] in the Padé approximation to the power series expansion.

A	$\bar{P} \cdot 10^{-2}$	σ
0.1	1.220243	$8 \cdot 10^{-7}$
0.2	2.410162	$6 \cdot 10^{-6}$
0.3	2.3120	0.004
0.4	2.14	0.11

Table 2: Convergence for periodic grating coupler analysis. \bar{P} is the average power in the -1st diffraction order, and σ is the standard deviation over the length of the power series ranging from 15 to 49.

A. This is shown in Table 2 illustrating that as we increase the amplitude of the surface relief, the standard deviation increases. However, even for an amplitude of 0.4, yielding a height-to-period ratio of the surface relief of more than one, the solution remains bounded with a reasonable error. We find that increasing the amplitude beyond 0.4, the scheme fails to converge.

It is worthwhile making another observation from Table 2, which clearly shows that there appears to be a maximum for the radiation into the -1st diffraction order. To analyze this, the power in the -1st order as a function of the grating height is shown in Fig. 2, confirming that, as expected, more

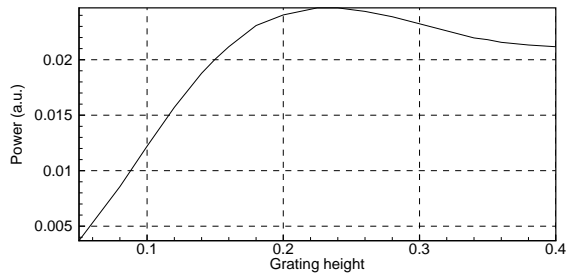


Figure 2: Power in -1st diffraction order as a function of the grating depth for a grating period of 0.7036 corresponding to perpendicular diffraction outcoupling. $\pi/2$.

power is radiated when the height of the surface relief grating is increased. However, the power has a maximum at a grating height of 0.23 above which the grating coupler becomes less efficient. A possible explanation is that when the surface relief becomes deep, the propagation of the guided wave in the thin film waveguide becomes heavily disturbed by the surface relief leading to a reduced coupling to the -1st diffraction order. Certainly, as we shall see for the focusing grating coupler, the nearfield radiation from a deep surface relief is severely distorted.

As another example we keep a fixed amplitude of $A = 0.1\lambda$ and consider the output power in the diffraction orders as a function of the grating period, Λ . Fig. 3 shows the power output in three diffraction orders, $m=-1$, -2 and -3 as a function of the grating period, and a number of things are worth noticing. First of all, we see that the -1st diffraction order has a global minimum for a grating period of $\Lambda = 1/1.4213$ corresponding to a perpendicular output. This is not surprising from a physical point of view because of the energy conservation. A second observation to be made is that

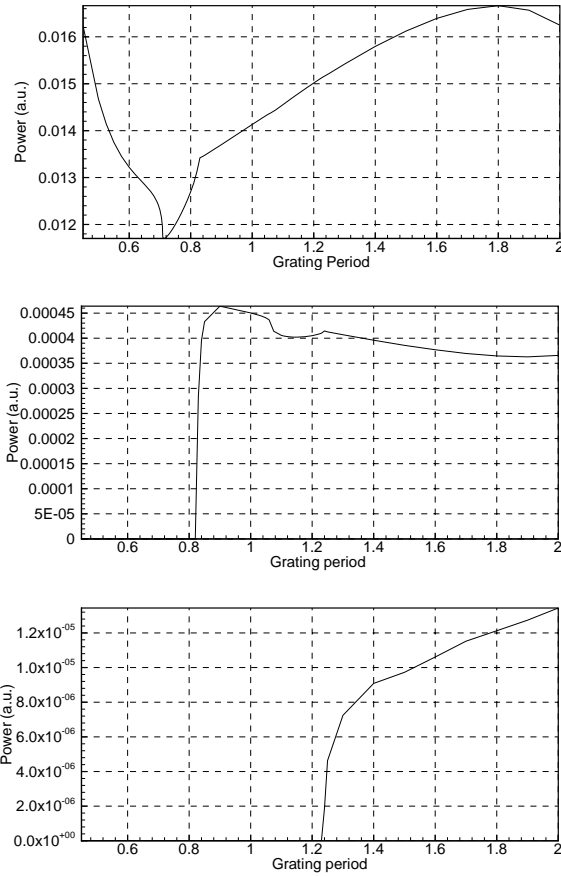


Figure 3: Power output in (a) -1st, (b) -2nd, and (c) -3rd diffraction order as a function of the grating period, Λ of the surface relief.

the appearance of a second diffraction order leads to an abrupt change in the slope of the curve of the first diffraction order. A similar change of slope is seen for the -2nd diffraction order at the cutoff for the -3rd diffraction order.

4 Focusing grating couplers

Let us now demonstrate the use of the proposed boundary variation method to study aperiodic surface-relief gratings couplers of finite length. Clearly, as we use the periodic Rayleigh series expansion for the radiated fields, the grating is implicitly forced to be periodic. However, as we shall demonstrate, choosing a sufficiently large total length of the computational domain as compared with the length of the finite surface relief, the results becomes consistent with those obtained using a method dealing with truly finite gratings.

For the FGC surface relief we use the generic profile

$$f_{\delta}(z) = A \exp \left[- \left(\frac{z - z_0}{w} \right)^2 \right] \cos [2\pi (a_0 + a_1 (z - z_0)) (z - z_0)] \quad (26)$$

where A is the amplitude, w is the width of the exponentially truncated relief, z_0 is the center of the relief, $a_0 = 1/\Lambda$ for the unchirped relief, and a_1 is the chirp parameter.

To establish the necessary length to simulate a FGC of finite extent, we investigate the farfield radiation pattern when varying the total length, L , of the computation domain. The number of modes in the Fourier transform is scaled with L to maintain a constant resolution. Fig. 4 shows the farfield radiation pattern for different values of L with the parameters for the surface relief being: $A = 0.25$, $a_0 = 1.4213$, $a_1 = 0.005$, and $w = 3$. From the figure it is clear that once the length of the computation domain exceeds 16, or around $5w$, the side-lobes caused by the periodicity are efficiently suppressed.

Another issue related to the Fourier transform is the resolution required to accurately resolve the structure of the surface relief, i.e. the number of terms in Eq. (12). To address this, we have performed a number of simulations with a varying resolution for the same geometry as discussed in the above. The results are illustrated in Fig. 5, where we find that once the number of Fourier modes exceeds $F = 26$ corresponding to a little more than 2 modes per wavelength for this case, the side lobes are efficiently suppressed and the center lobe well resolved. It should be noted that the

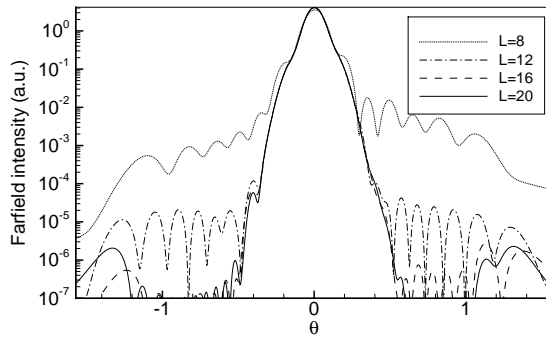


Figure 4: Farfield radiation pattern for different length of the computational domain, L .

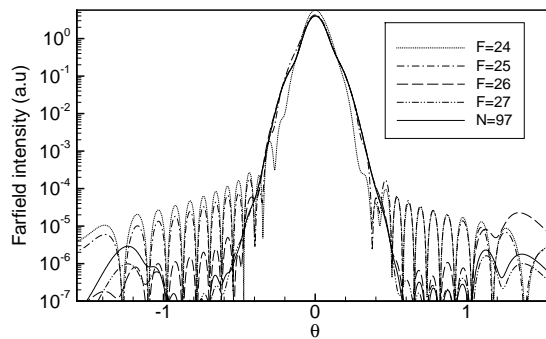


Figure 5: Farfield radiation pattern for varying resolution used in the Fourier series, Eq. (12), to represent the surface relief.

Fourier spectrum of the surface relief is affected by both the width of the Gaussian truncation and the chirping of the grating period so that a higher resolution may be necessary for other values of these parameters.

Having established resolution and computational domain requirements for our problem, let us perform a direct comparison with a highly accurate spectral collocation (SC) method[6]. This method computes a rigorous solution of the vectorial time-domain Maxwell equations, and we have previously demonstrated its superior accuracy [13].

For the comparison, we study a longer FGC. The total length of the computation domain is now 80λ , $w = 12\lambda$, $a_0 = 1.4213$, $a_1 = 0.01$, and $A = 0.3$ yielding a height-to-period ratio close to one. As is seen in Fig. 6

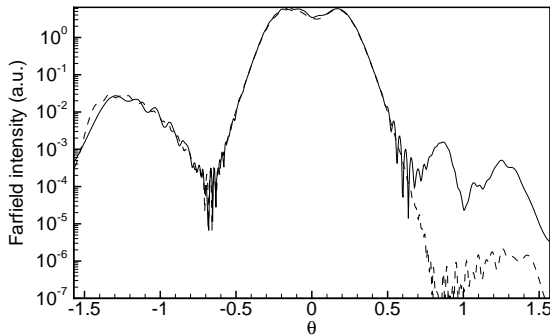


Figure 6: Farfield radiation patterns for FGC computed using the boundary variation method (dashed) and the spectral collocation method (solid).

that there is an excellent agreement between the farfield patterns of the two methods even for this relatively deep surface relief grating.

To further validate the proposed approach, we compute a number of solutions using both the BV and the SC methods and compared the nearfield solutions. Fig. 7 shows a line scan of the intensity in the focal plane for both methods for three different values of the surface relief amplitude and Table 3 lists key figures for the simulations. The computations were performed on a single-processor Sun Ultra-1 workstation.

We find excellent correspondence in the farfield maintained in the nearfield even though the intensity is slightly lower for the BV method for all amplitudes, which may be due to not accounting for multiple reflections. We also confirm that the use of deep surface reliefs leads to a deteriorated outcoupling from the waveguide grating coupler: While, it is clear that for $A = 0.1$

A	M		f		time	
	BV	SC	BV	SC	BV	SC
0.1	7	47.1	47.0	46s	30h	
0.2	13	46.3	46.2	390s	64h	
0.3	17	45.2	45.1	1081s	126h	

Table 3: Key figures for spectral collocation (SC) and the proposed boundary variation (BV) computations. A is the amplitude of the surface relief. An $[M, M]$ Padé approximant is used for the BV method. f is the focal length normalized with the free-space wavelength, and time reflects the total computation time.

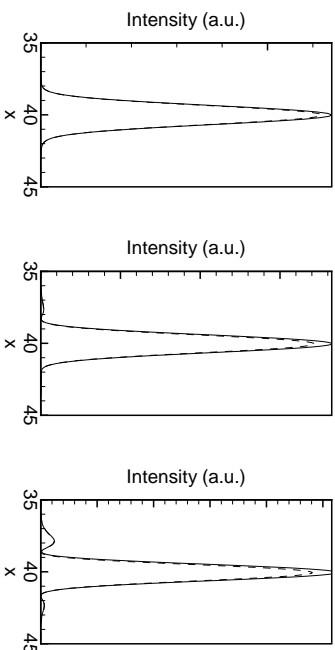


Figure 7: Nearfield radiation patterns for surface relief amplitudes (a) 0.1, (b) 0.2, and (c) 0.3 using the boundary variation method (dashed) and the spectral collocation (solid) methods.

the intensity is symmetric and Gaussian in the focal plane, we find that as the amplitude increases to $A = 0.2$ and $A = 0.3$ side-lobes evolves and an asymmetry becomes noticeable. We also see a shift in the focal plane, Table 3, towards the surface relief for both methods which agree well on the focal length. These conclusions are also consistent with computations using the FDTD method[14].

Looking at the computation time in Table 3, it is evident that the use of the approximate boundary variation method certainly pays off: While we find excellent agreement with the rigorous spectral collocation method, we find a reduction in the computation time exceeding a factor of 2000 is achievable, a fact which calls for the future use of the method as the forward solver in an optimization scheme.

5 Conclusions

We have presented the development of a boundary variation method for the analysis of both periodic and aperiodic waveguide grating couplers and given examples of the analysis of continuous surface relief gratings. For a periodic grating, we have found that the power radiated into the fundamental -1st diffraction order does not increase monotonically with the grating height. Rather an optimum exists and we attribute this to the distortion of the guided wave propagation resulting from very deep surface reliefs.

For a focusing grating coupler, we have found excellent agreement with the highly accurate spectral collocation method. A reduction in computation time of up to more than 2000 times compared to a rigorous approach is achieved.

These very encouraging results suggest that further development along the lines discussed here are worthwhile and we are currently considering the formulation of the boundary variation based methods for the 3-D forward scattering problem.

6 Acknowledgments

Oscar Bruno and Fernando Reitich are gratefully acknowledged for fruitful discussions on the boundary variation method. JSH wishes to acknowledge the partial support for this work by DARPA/AFOSR Grant F49620-1-0426.

References

- [1] T. K. Gaylord and M. G. Moharam, "Analysis and applications of optical diffraction by gratings," *Proc. IEEE*, vol. 73, pp. 894–937, 1985.
- [2] B. Lichtenberg and N. C. Gallagher, "Numerical modeling of diffractive devices using the finite element method," *Opt. Eng.*, vol. 33, pp. 1592–1598, 1994.
- [3] K. Hirayama, E. N. Glytsis, T. K. Gaylord, and D. W. Wilson, "Rigorous electromagnetic analysis of diffractive cylindrical lenses," *J. Opt. Soc. Am. A*, vol. 13, pp. 2219–2231, November 1996.
- [4] D. W. Prather and S. Shi, "Formulation and application of the finite-difference time-domain method for the analysis of axially symmetric diffractive optical elements," *J. Opt. Soc. Am. A*, vol. 16, pp. 1131–1141, May 1999.
- [5] K. H. Dridi and A. Bjarklev, "Optical electromagnetic vector-field modeling for the accurate analysis of finite diffractive structures of high complexity," *Applied Optics*, vol. 38, pp. 1668–1676, March 1999.
- [6] J. S. Hesthaven, P. G. Dinesen, and J.-P. Lynov, "Spectral collocation time-domain modeling of diffractive optical elements," *Journal of Computational Physics*, vol. 155, pp. 287–306, 1999.
- [7] O. P. Bruno and F. Reitich, "Numerical solution of diffraction problems: a method of variation of boundaries," *J. Opt. Soc. Am. A*, vol. 10, pp. 1168–1175, June 1993.
- [8] O. P. Bruno and F. Reitich, "Numerical solution of diffraction problems: a method of variation of boundaries. II. finitely conducting gratings, padé approximants, and singularities," *J. Opt. Soc. Am. A*, vol. 10, pp. 2307–2316, November 1993.
- [9] O. P. Bruno and F. Reitich, "Numerical solution of diffraction problems: a method of variation of boundaries. III. doubly periodic gratings," *J. Opt. Soc. Am. A*, vol. 10, pp. 2551–2562, December 1993.
- [10] S. Ramo, J. R. Whinnery, and T. van Duzer, *Fields and waves in communications electronics*. John Wiley & Sons, 3rd ed., 1993.

- [11] O. Bruno and F. Reitich, "Solution of a boundary value problem for helmholtz equation via variation of the boundary into the complex domain," *Proc. Royal Soc. of Edin.*, vol. 122A, pp. 317–340, 1992.
- [12] S. A. Schelknuoff, "Some equivalence theorems of electromagnetics and their application to radiation problems," *Bell Systems Technical Journal*, vol. 15, pp. 92–112, 1936.
- [13] P. G. Dinesen, J. S. Hesthaven, J. P. Lynov, and L. Lading, "Pseudo-spectral method for the analysis of diffractive optical elements," *J. Opt. Soc. Am. A*, vol. 26, pp. 1124–1130, May 1999.
- [14] P. G. Dinesen and K. H. Dridi, "Spectral collocation and fdtd approaches for the design of focusing grating couplers," *submitted to J. Opt. Soc. Am. A*, 2000.